Ryszard KLEMPKA, Bogusław ŚWIĄTEK

Akademia Górniczo-Hutnicza, Wydział Elektrotechniki, Automatyki, Informatyki i Elektroniki

Active Power Filter Controllers based on Artificial Intelligence

***Abstract**. An ever-growing share of non-linear loads, mainly electronic and power electronic equipment, results in an increase of values non-active currents in the power supply network. A reactive component of fundamental frequency and high-order harmonics can be distinguished in these loads current. Estimation of their values and their subsequent elimination is the objective of an active power filter (APF). Various filter control algorithms of different extent of complexity and immunity to disturbances have been proposed in a great number of papers. This paper presents conception of two different algorithms of a single phase APF filter control. The first control algorithm in which the estimation of a non-active current component waveform and VSI converter transistors control are performed by means of neural networks (ANN). The second control algorithm employs genetic algorithm. It ensures high quality of performance as measured by distortion level of the source current, using no greater number of switching operations in a converter, within one line voltage cycle, than a given limit value. Due to the above the switching losses can be reduced and the system efficiency increased.*

Streszczenie.** Rosnący udział odbiorników nieliniowych, głównie sprzętu elektronicznego i energoelektronicznego, prowadzi w konsekwencji do wzrostu wartości prądów nieaktywnych w sieci zasilającej. W prądzie tych odbiorników można wyróżnić składową bierną o częstotliwości podstawowej oraz wyższe harmoniczne. Estymacja ich wartości oraz następnie ich eliminacja jest celem działania filtrów aktywnych (APF). W licznych artykułach zaproponowano różne algorytmy sterowania filtrów, charakteryzujące się różnym stopniem złożoności i różnym stopniem odporności na zakłócenia. W niniejszym artykule przedstawiono koncepcję dwóch algorytmów sterowania jednofazowego APF W pierwszym algorytmie zarówno estymacja przebiegu czasowego nieaktywnej składowej prądu, jak również sterowanie tranzystorami przekształtnika VSI realizowane jest za pomocą sieci neuronowych (ANN). Drugi algorytm sterowania wykorzystuje Algorytm Genetyczny. Gwarantuje on wysoką jakość działania mierzoną stopniem odkształcenia prądu źródła zasilania, będzie realizowane za pomocą liczby przełączeń w przekształtniku w okresie napięcia nie większej niż zadana wartość graniczna.* W związku z powyższym straty przełączania można zmniejszyć a wydajność systemu wzrasta. (Sterowanie energetycznym filtrem aktywnym oparte na sztucznej inteligencji***)

Keywords: Active power filter, Neural Networks, Genetic Algorithms.
Słowa kluczowe: Filtr aktywny, sieci neuronowe, algorytm genetyczny.

1. Active Power Filter with Neural Network controller

Schematic diagram of the active power filter arrangement is shown in Fig. 1. The single-phase source of sinusoidal voltage U_s of amplitude U_{max}= 110[V] and inductive reactance X_s= 1,1 [mH], which is a sum of source and feeding line reactance, is loaded with nonlinear thyristor bridge and R_L, L_L branch (R_L=10[Ω], L_L=2[mH]). The active filter consists of the capacitor bank C (C=2[mH]), reactor L_1 (L_1=7 [mH]) and power electronic converter T_1-T_4. The converter comprises intelligent power module (IPM) of Mitsubishi type PM20CSJ060 with ratings U_N=600[V], I_N= 20[A], f=20 [kHz].The capacitor voltage is maintained constant U_{DC}=170 [V] by means of the filter control circuit. The source voltage and current, the load current, the filter current and the filter capacitor voltage were measured using LEM transducers.

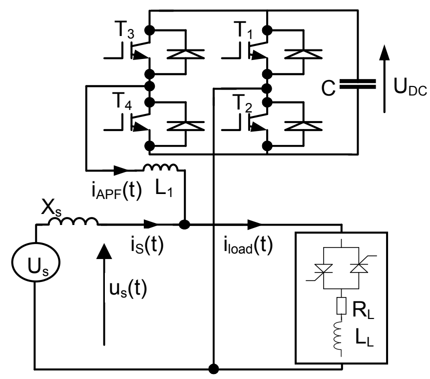

Fig.1. Schematic diagram of the active power filter laboratory arrangement

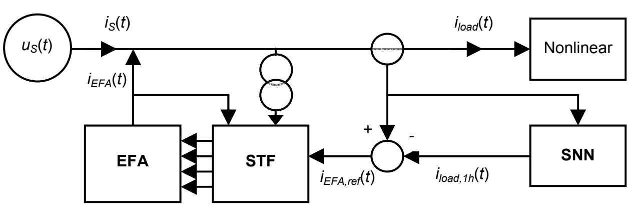

Fig. 2: Block diagram of the control system

Various filter control algorithms have been proposed in a great number of papers [1]-[7]. The filter control system has been developed using the dSPACE system and artificial neuron networks (SSN) have been employed to estimate the waveforms of non-active component of the load current. The filter control system (Fig. 2) contains two main blocks:

- SSN block for determination of the reference current using artificial neuron networks
- STF block for the control of the filter converter transistors. STF generates gate pulses for T_1 – T_4 transistors.

The SSN block operation consists in decomposition of the load current into Fourier series and determination of the filter reference current according to the following relation:

(1) $$i_{EFA,ref}(t) = i_{load}(t) - I_{load,1h} \sin \omega t$$

where: $I_{load,1h}$ – amplitude of the first harmonic of the load current

Detailed description of the block operation can be found in [8], [9].

Using the reference current signal and the source voltage waveform STF block generates gate pulses for transistors according to the following algorithm:

if $i_{EFA,ref}(t) \geq 0$ **then**

if $i_{EFA}(t) > i_{EFA,ref}(t)$ **then** $T_{1..4}$ = 0
else $T_{2,3}$ = 1

if $i_{EFA,ref}(t) < 0$ **then**

if $i_{APF}(t) > i_{APF,ref}(t)$ **then** $T_{1,4}$ = 1
else $T_{1..4}$ = 0

The simulink model of the system with a passive filter added to the arrangement is shown in Figure 3.

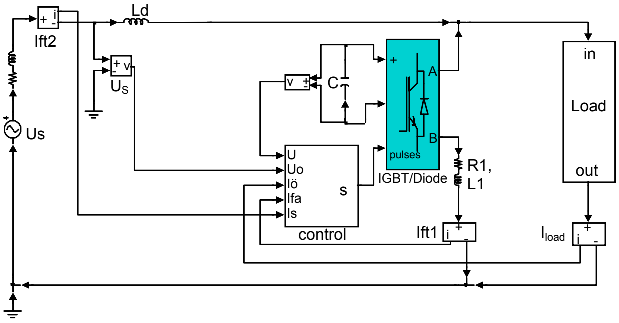

Fig. 3. The simulink model of the system

The results of laboratory tests, in the form of the source voltage and current oscillograms are shown in Fig. 3. Fig. 3a shows the waveforms of the source voltage and current without the filter, and Fig. 3b shows the same quantities in the circuit with the filter, being controlled according to the algorithm above. The measurement was performed under the same load conditions. During rapid change in the load current, a distortion of significant amplitude occurs in the source sinusoidal current (Fig. 3b).

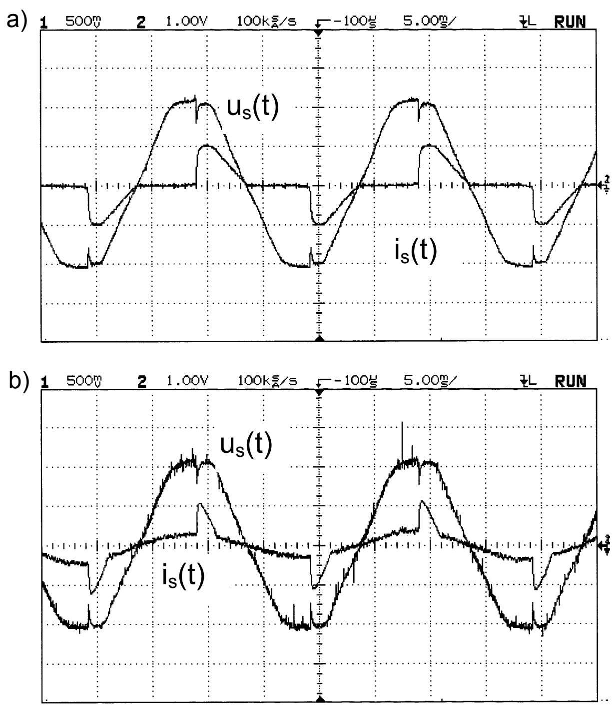

Fig. 4 The source voltage and current waveforms (1division =100 (V), =10(A))

2. Estimation of the load current using adaptive neural network

Solution for load current estimation, presented in [10] was based on measuring the samples contained in a time-window, one cycle of the voltage waveform wide. This algorithm was not enough efficient as it needed ca. 55 μs for calculations to be performed. An adaptive linear neuron, trained according to Wirof-Hoff's algorithm, is presented below. Harmonics assessment in this method is based on a single measurement in each step of iteration. The load current, given periodicity of the waveform, could be transformed into Fourier series:

$$i_{load}(t) = \sum_{h \in N} \left(I_{Ph} \sin(h\omega t) + I_{Qh} \cos(h\omega t) \right) \tag{2}$$

where N is a set of the harmonics taken into account. In terms of vector notation the expression (2) could be represented as:

$$i_{load}(t) = \mathbf{W}^T \mathbf{x}(t) \tag{3}$$

where:

$\mathbf{W}^T = [I_{P1}, I_{Q1} \ldots I_{Ph}, I_{Qh} \ldots]$;

$\mathbf{x}(t) = [\sin(\omega t, \cos(\omega t) \ldots \sin(h\omega t, \cos(h\omega t) \ldots]^T$.

This notation is equivalent to the expression, which describes response of a single linear neuron to sine and cosine function values applied to its input in subsequent discrete time instants corresponding with the current sampling time $i_{load}(t)$ (Fig. 5). Weight factors of this neuron correspond to the amplitudes of the measured current harmonics.

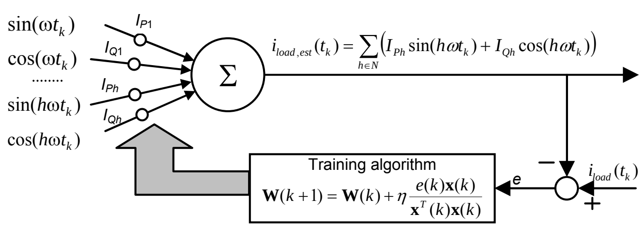

Fig. 5. Diagram of adaptive linear neuron

The purpose of the estimation is determining the current first harmonic, in phase with the source voltage. In order to ensure synchronisation of the estimated current component with the source voltage, time is assumed $t_k = 0$ at the instant of changing the voltage value from positive value to negative, and increases with a step equal to the sampling interval T_p ($t_k = t_k + T_p$) until next identical change. The training process consists in modification of weight factors ***W*** so as the ANN response be as close as possible to the measured value of $i_{load}(t)$ by employing the Widrof-Hoff's algorithm, which consists in minimisation by means of the steepest descent method of the function (4) being a squared difference between the measured load current and the current estimated by the neuron:

$$Q = \left(i_{load}(t_k) - \sum_{h \in N} \left(I_{Ph} \sin(h\omega t) + I_{Qh} \cos(h\omega t) \right) \right)^2 = e^2 \tag{4}$$

we get:

$$\mathbf{W}(k+1) = \mathbf{W}(k) + \eta \frac{e(k)\mathbf{x}(k)}{\mathbf{x}^T(k)\mathbf{x}(k)} \tag{5}$$

where scalar product $\boldsymbol{x}^T\boldsymbol{x}$ normalizes the neuron input vector, and η is the network learning rate. While executing one step of the algorithm over the sampling interval the weight factors, and thus harmonics amplitudes, are determined in a time shorter than one cycle of the voltage waveform.

3. VSI bridge transistors control

The rule of filter control is achieved in the course of learning process of unidirectional neural network. The purpose of the neural network is to switch the bridge transistors S_1-S_4 on and off (Fig. 1) in such a manner that under the resulting voltage across the input inductance L_1 the current would differ as little as possible from the reference current

$i_{APF,ref}(t)$. This voltage depends on the actual value of the current i_{APF}(t), the reference current and the load voltage, as follows from a voltage equation (6) for the circuit in Figure 6.

$$u_{load}(t) = u_{APF}(t) + L_1 \frac{di_{APF}(t)}{dt} + i_{APF}(t) R_1 \tag{6}$$

Transforming to differential form:

$$u_{APF}(k) = f\left(i_{APF}(k), u_{load}(k), i_{APF,ref}(k+1)\right) \tag{7}$$

where: $i_{ref,APF}(k+1) = i_{APF}(k+1)$

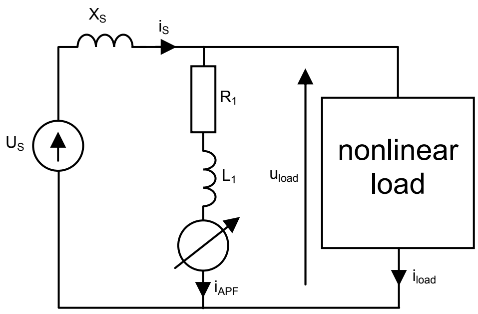

Fig. 6 Equivalent circuit diagram: power supply network – nonlinear load – APF;

For each value of the voltage u_{APF} is assigned a state of bridge's transistors, and therefore relevant unipolar values of neural network outputs. In training process the neural network shall find out the relation:

$$[y_1, y_2, y_3, y_4] \Rightarrow u_{APF}(k) = f\left(i_{APF}(k), u_{load}(k), i_{ref,APF}(k+1)\right) \tag{8}$$

where: [y_1, y_2, y_3, y_4] – neural network outputs which are gate signals for the transistors.
Training of ANN requires a training set, which consist of two matrices:

$$\mathbf{P} = \left[i_{APF}(k), u_{load}(k), i_{ref,APF}(k)\right]^T \tag{9}$$

$$\mathbf{T} = \left[y_1(k), y_2(k), y_3(k), y_4(k)\right]^T \quad k=1 \dots N \tag{10}$$

a)

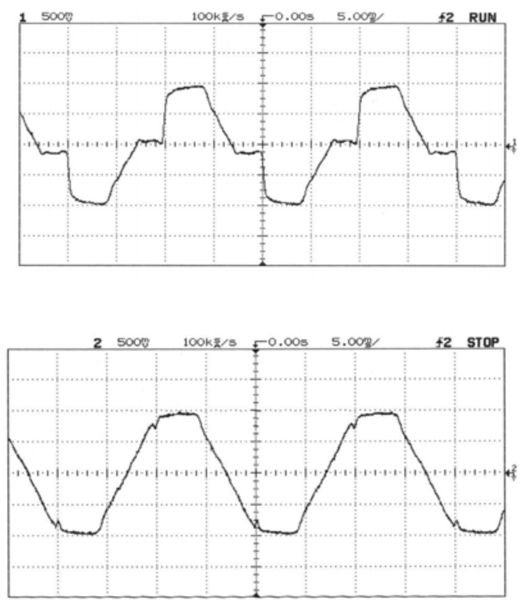

b)

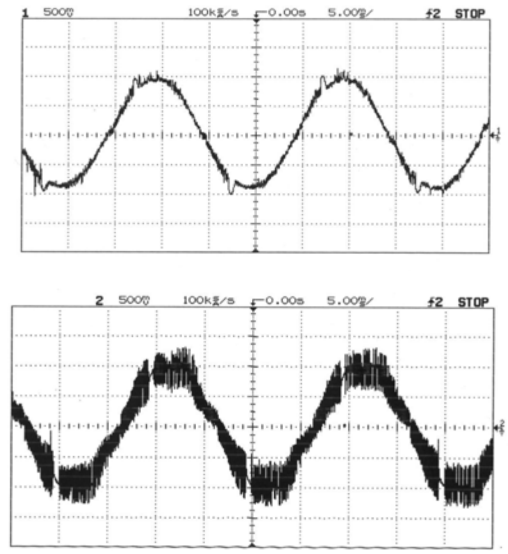

Fig. 7. The source current and voltage waveforms before (a) and after (b) addition of the active filter

Neural network learns by changing the weight factors assigned to individual inputs in such a way that it minimises the objective function:

$$Q = \frac{1}{2} \sum_{k=1}^{N} \left[\sum_{i=1}^{4} \left(T_i(k) - y_i^{(K)}(k) \right)^2 \right] \tag{11}$$

where: $T_i(k)$ – desired outputs of the neural network, $y_i^{(K)}(k)$ - calculated ANN outputs.

4. Laboratory tests

The results of the laboratory tests in the form of oscillograms of the source current and voltage are shown in Fig 7. (in Fig.7a – without filter and in Fig.7b - with filter controlled according to above mention algorithm). The measurements were performed under the same load conditions. In case of a rapid change in the load current a distortion of significant amplitude in comparison with sinusoidal shape occurs in the waveform of the source current.

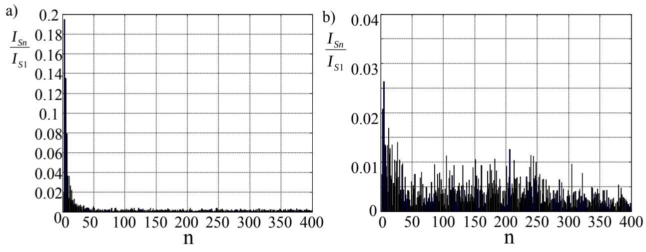

Fig. 8: The source current amplitude spectrum before (a) and after (b) the addition of the active filter.

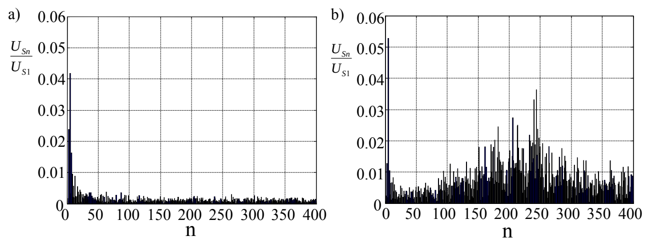

Fig. 9: The source voltage amplitude spectrum before (a) and after (b) the addition of the active filter

The values of THD_I and THD_U network factors are respectively 26,6% and 6% before addition of the active filter and 10,3% and 18,7% after the addition of the active filter. The source current and voltage spectra before and after the addition of the active filter are shown in Fig. 8 and Fig. 9.

The filters unload the power sources and feeding lines from flowing of the reactive component and harmonics generated mainly by power electronic converters. The source current contains high-frequency component created by the action of the filter switches according to the principle of active filter operation. That component is responsible for the distortion of the source voltage because of non-zero internal inductive reactance of actual power sources and transmission lines. Passive filters are employed in order to unload power sources and feeding lines from flowing of currents having filter switches action frequency and its multiplicity [11].

The source current and voltage waveforms together with their frequency spectra after the addition of the designed passive filter are shown in Fig. 10 and Fig. 11.

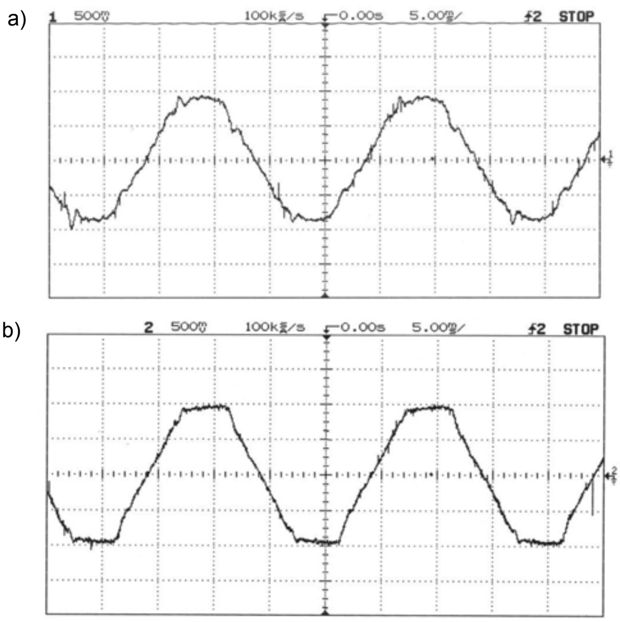

Fig. 10: The source current (a) and voltage (b) oscillograms after the addition of the designed passive filter.

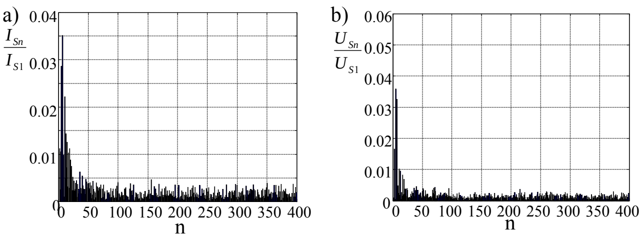

Fig. 11: The current (a) and voltage (b) spectra recorded in the real power system after the addition of the designed passive filter

The values of THD_I and THD_U factors of the recorded signals are respectively 7,3% and 6,3%. The diagrams in Fig. 10 and Fig. 11 testify to the proper selection of the parameters of the C-filter. The THD factors have been considerably reduced but their values are still not satisfactory.

5. Control algorithm based on genetic algorithm

One of control algorithm of power active filter can be a control, which employs the genetic algorithm. It ensures high quality of performance as measured by distortion level of the source current, using no greater number of switching operations in a converter, within one line voltage cycle, than a given limit value. Due to the above the switching losses can be reduced and the system efficiency increased [12].

The control goal is the determination of the switching pattern for switches S_1-S_4 (Fig. 1), which can ensure the required shape of the filter current. For the majority of controls the larger the number of switching operations during the line voltage cycle, the better the obtained result. This cause an increase in switching losses and, for instance, in the systems with hysteresis controllers and narrow hysteresis band may result in exceeding the permissible switching frequency for applied semiconductor devices.

Thus, we are dealing with the optimisation of two mutually exclusive goals: minimization of the source current distortion and minimization of the number of switching operations during the voltage cycle.

The purpose of the optimisation, using genetic algorithm is to find such a switching control sequence for the active filter (Fig. 3) under consideration, that:

- the line current be as close as possible to the reference waveform i.e. to the fundamental harmonic of the source current,
- the number of switching operations during the voltage cycle will not exceed given limit value.

The genetic algorithms operate on a population of solutions, which are subject to assessment. On the basis of this assessment the selection and reproduction of individuals is performed and the population improves. Therefore, in terms of the statistics, in the next generation the sequence of switches states should generate the line current better approximating the first harmonic than the former generation.

In this application of the genetic algorithm the population was 20 individuals and the length the code sequence represented the states of the S_1 switch. The states of the switch S_4 were assumed identical to those of the switch S_1. The states of the switches S_2 and S_3 are identical and they are negation of the switch S_1 states.

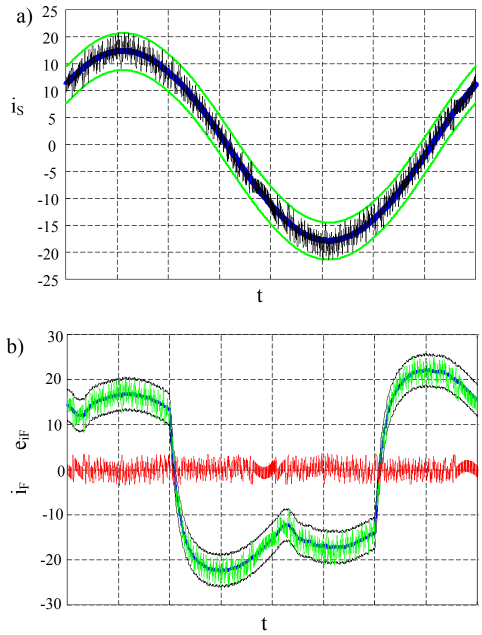

Fig. 12. The waveforms of the line current and the line current first harmonic (a), the waveforms of the filter current and its error (b)

The solution generated by the genetic algorithm is assessed by means of simulation using the Matlab package. Results of simulation are the waveforms of: the line current and difference of the line current first harmonic and the load current. This difference is the current, which should flow through the filter. The genetic algorithm minimizes this difference. The quality index is the number of the switches states, which generate error of the current with respect to the first harmonic waveform, smaller than the given permissible error. The more is such “good” states of the switches, the fitter, the better, is the individual.

Figure 12a show the waveforms of the line current and of the difference of the line current first harmonic and the load current after the optimisation, using genetic algorithm under the assumption that the error of the first harmonic reproduction (e_{max}) shall not be greater than 3.5A, and the maximum number of switching does not exceed 800. As seen from the graphs, the solution satisfies the requirements. The genetic algorithm has found correct states of the control switches. The waveforms of the filter current and its error shown in Fig. 12b.

6. Conclusion

The simulation and experimental research have proved that the procedures of the reference current estimation and bridge transistors control are correct. To minimize the harmonic content of the work resulting from APF transistor switches must be used for passive broadband filter. Further work is aimed on reduction of estimation errors of the current components and application of algorithm for three-phase APF control.

The active filter controlled by neural network also has the disadvantage that could not be completely removed. There were moments when the filter does not work properly. This defect was devoid of the genetic algorithm-controlled filter, which has, however, other disadvantages. A disadvantage of this solution is that a change in the system parameters, or a character of the load will result in an erroneous filter operation. The selected states of switches are adequate only for the system static state. This inconvenience can be remedied by employing a supervisory control algorithm. Another solution is the use of the determined solution as the training sequence for a neural network, which should manage with dynamic states.

REFERENCES

[1]. Gonzales-Romera E., Romero-Cadaval E., Ruiz-Arranz S., Milanes-Montero M., Ogólna poprawa jakości energii w sieci dystrybucyjnej energetycznymi filtrami aktywnymi. Optymalizacja rozmieszczenia i strategii, *Przegląd Elektrotechniczny* 01a/2012, 51-55

[2]. Sozański K., Układ sterowania energetycznym filtrem aktywnym z zastosowaniem zmodyfikowanego algorytmu opartego na teorii mocy chwilowej, *Przegląd Elektrotechniczny* 01/2011, 96-100

[3]. Adrikowski T., Buła D., Pasko M. Symulacja filtru aktywnego ze sterowaniem predykcyjnym w środowisku MATLAB i OrCAd, *Przegląd Elektrotechniczny* 05/2011, 1-5

[4]. Adrikowski T., Buła D., Pasko M., Współpraca energetycznego filtru aktywnego z filtrem hybrydowym w przypadku symetrii obciążenia, *Przegląd Elektrotechniczny* 05/2011, 25-28

[5]. Płatek T., Stabilność systemu zasilania z równoległym filtrem aktywnym zapewniającym kompensację pojemnościowej mocy biernej, *Przegląd Elektrotechniczny* 12a/2011, 173-177

[6]. Wojciechowski D., Układ sterowania równoległym filtrem aktywnym ze sprzęgającym obwodem LCL, *Przegląd Elektrotechniczny* 02a/2010, 65-70

[7]. Marian Pasko , Dawid Buła, Hybrydowy energetyczny filtr aktywny w układzie z filtrem pasywnym dla jednej harmonicznej, Przegląd Elektrotechniczny 03/2010, 205-210

[8]. Kosiorowski St., Świątek B.: Active Power Filter (APF) Using an Additional Reactor, 10th International Power Electronics and applications, EPE 2003, Toulouse.

[9]. Świątek B., Hanzelka Z.: Neural Network-Based Controller for an Active Power Filter. 10th International Power Electronics and Motion Control Conference, 2002, Dubrovnik

[10]. Świątek B., Hanzelka Z. A Single-phase Active Power Filter with Neural Network-Based Controller. IASTED International Conf. Power and Energy Systems, July 3-6, 2001, Rhodes, Greece.

[11]. Świątek B., Klempka R., Kosiorowski S., Minimization of the source current distortion in systems with single-phase active power filters and additional passive filter designed by genetic algorithms, 11th European Conference on Power Electronics and Applications, EPE2005, 11-14 September 2005, Dresden

[12]. Klempka R., Hanzelka Z., Active filter control by genetic algorithms, 3rd International Workshop Compatibility in Power Electronics, CPE 2003, 28-30 May 2003, Gdańsk-Zielona Góra.

Autorzy

dr inż. Ryszard Klempka, Akademia Górniczo-Hutnicza, Wydział Elektrotechniki, Automatyki, Informatyki i Elektroniki, al. Mickiewicza 30, 30-059 Kraków, e-mail: klempka@agh.edu.pl

dr inż. Bogusław Świątek, Akademia Górniczo-Hutnicza, Wydział Elektrotechniki, Automatyki, Informatyki i Elektroniki, al. Mickiewicza 30, 30-059 Kraków, e-mail: boswiate@agh.edu.pl

The correspondence address is:
klempka@agh.edu.pl